Mon. Not. R. Astron. Soc. **348,** 279–284 (2004)

Mid-infrared polarimetry and magnetic fields: an observing strategy

D. K. Aitken,[1⋆] J. H. Hough,[1] P. F. Roche,[2] C. H. Smith[3] and C. M. Wright[3]

[1]*Division of Physical Sciences, University of Hertfordshire, College Lane, Hatfield, Herts AL10 9AB*
[2]*Department of Astrophysics, Oxford University, Keble Road, Oxford OX1 3RH*
[3]*School of Physics, University College, ADFA, UNSW, Canberra, ACT 2600, Australia*

Accepted 2003 October 24. Received 2003 October 24; in original form 2003 September 1

ABSTRACT

Linear polarimetry in the mid-infrared can be used to obtain magnetic field directions in astronomical sources. However, since the polarization can arise from emission and/or absorption from aligned grains, care is needed to plan observations so that enough information is obtained to identify and separate the components of polarization. Procedures for doing this from spectropolarimetry, and from polarimetric imaging at a minimum of two wavebands and making an appropriate filter choice, are presented here, together with an example.

Key words: magnetic fields – polarization – methods: observational – techniques: polarimetric – dust, extinction – infrared: ISM.

1 INTRODUCTION

With the recent deployment of 8-m class telescopes, many of which are optimized for the thermal infrared, and the accessibility of mid-infrared array imager/spectrometers with polarimetric capabilities, there will be an increasing ability to investigate magnetic field directions through spectropolarimetry and polarimetric imaging in the mid-infrared. A particular characteristic of the mid-infrared is that linear polarization due to aligned grains can be by either emission or absorption, or both, and these processes separately yield a polarization that differs by 90° for the same grain alignment. This paper describes an observing strategy to separate and identify these components in most situations.

The information on magnetic field directions that polarimetry can give is independent of the details of grain alignment for the following reasons: In equilibrium with ambient gas, dust grains spin about a short axis with rotational frequencies in the range 10^5–10^6 Hz; as a consequence they develop a magnetic moment through the Barnett effect (Landau & Lifshitz 1960) and their spin axes precess about the ambient field direction (Dolginov & Mytrophanov 1976). In an isotropic distribution there are no preferred precession angles, so that this does not constitute alignment, but the typical precession period, of the order of days, is many orders of magnitude shorter than any of the other processes that affect the grain spin. Consequently, any disturbance to isotropy results in a net spin orientation either along or normal to the ambient field, and grain emission will be polarized normal to or along the field. In practice, most disturbance mechanisms align the spins along the field so that grain emission will be polarized normal to the field projection, and where an observational check is possible it appears that there is no exception to this. Similarly, if the grains are cold and absorb, the polarization of the transmitted radiation will be parallel to the field projection on the sky. If both warm and cold grains are present along the line of sight, then the observed polarization will be a combination of the two; observationally this situation is often revealed by a wavelength-dependent position angle, which indicates more than one polarization mechanism and probably a change in field direction.

If observations are for the determination of field directions, it is clearly necessary to identify whether grains in absorption or emission are producing the polarization. Fortunately emission and absorption have significantly different polarization spectra, which enables their identification, and, when both processes contribute along the line of sight, a simple two-component model can be used to separate the contributions.

Such separations have been done when spectropolarimetry in the 10-μm window is available (Aitken 1996; Smith et al. 2000, hereafter SWARH), and the details of this procedure are given in Section 2.1. The method relies on the well-known shape of the polarization feature in the 8–13 μm region and might eventually be applied to the 20-μm feature as well, but at present this, and its relation to that at 10-μm, is poorly understood, largely because of the paucity of data (e.g. SWARH).

It is also possible to identify and separate the components from photopolarimetry alone given observations made at two or more wavelengths (a check on validity would require at least three), and we present an algorithm for doing this in Section 2.2.

Note that observations at a single wavelength in the mid-infrared give no indication as to whether polarization is due to emission or absorption, or both, and consequently is only of use in studies of magnetic field directions given some other qualifying information. Submillimetre observations generally have no such ambiguity as the polarization is always in emission.

2 METHOD

Since this paper is about observational matters, some general procedural comments may be in order. Mid-infrared polarizations rarely

⋆E-mail: dka@star.herts.ac.uk

exceed 10 per cent and are frequently only a few per cent or less. Consequently, meaningful polarimetry requires observations to an accuracy of a fraction of one per cent and the minimization of effects that can cause spurious polarizations.

Many instrumental components are polarization-sensitive (e.g. gratings, detectors) and a typical practice is to rotate the incoming polarization with a half-wave plate and use a fixed analyser to select a constant polarization to such elements and present a constant polarization to the detector(s).

In polarimetry, the most critical measurement is the difference between the intensity in orthogonal planes of polarization. In the presence of varying atmospheric transmission and emission, by far the best practice is to measure orthogonal components of polarization at the same time. This requires an appropriate beam splitter, such as a Wollaston prism, and two detectors or separation on an array. Orthogonal polarizations at 45° to this are then found from a rotation of the wave plate. In the mid-infrared Wollastons give only a small beam separation, which will not be adequate for extended sources of more than a few arcsecond size; it may be possible to use an angled wire grid analyser and two arrays. Unfortunately, any of these capabilities are rarely available for the mid-infrared, and one must then resort to sequential measurements of orthogonal polarizations, which need to be made at the shortest interval practicable.

2.1 Spectropolarimetry

Using a Wollaston with the slit aligned with the ray separation axis, spectra of orthogonal polarizations can be separated and measured at the same time. Failing this, choice of slit width can minimize seeing and pointing errors in sequential measurements.

In the mid-infrared, roughly from 7 to 25 μm, most polarization observed to date appears to arise from silicate-like grains and show spectral features in both intensity and polarization near 10 and 20 μm (SWARH). However, water and CO ice features near 3 and 5 μm do display polarization signatures, and polarization from such mantles might be expected in the mid-infrared. There is little evidence of polarization either from the polycyclic aromatic hydrocarbon (PAH) features seen in emission or from other identifiable components. Less than 10 per cent of sources in SWARH are inconsistent with silicate-like grains.

For absorption, the fractional polarization in the x direction is

$$p_{\rm a} = \frac{{\rm e}^{-\tau_x} - {\rm e}^{-\tau_y}}{{\rm e}^{-\tau_x} + {\rm e}^{-\tau_y}} = -\tanh\left(\frac{\Delta\tau}{2}\right) \simeq -\frac{\Delta\tau}{2} \qquad 2.1$$

to the approximation that $\Delta\tau/2 = (\tau_x - \tau_y)/2$ is small, while the negative sign indicates that the polarization is in the direction of least extinction. For optically thin emission, the fractional polarization is

$$p_{\rm e} = \frac{\tau_x - \tau_y}{\tau_x + \tau_y} = \frac{\Delta\tau/2}{\tau} \simeq -\frac{p_{\rm a}}{\tau}.$$

We have taken the absorptive profile, $f_{\rm a}(\lambda) = p_{\rm a}(\lambda)/p_{\rm a}(\lambda_{\rm max})$, as that of the Becklin–Neugebauer (BN) object in Orion (Aitken, Smith & Roche 1989), not only because this is the best-defined spectral feature but also because it closely resembles many other sources that are consistent with absorptive polarization alone (e.g. SWARH).

So far there has been little spectropolarimetry of sources with purely emissive polarization: in SWARH there are only two cases where this assignment has been made (NGC 1068 and RCW38) and the data quality is not good enough to define a spectral form for emissive polarization. Failing this, we form the emissive polarization profile from

$$p_{\rm e} \simeq p_{\rm a}/\tau$$

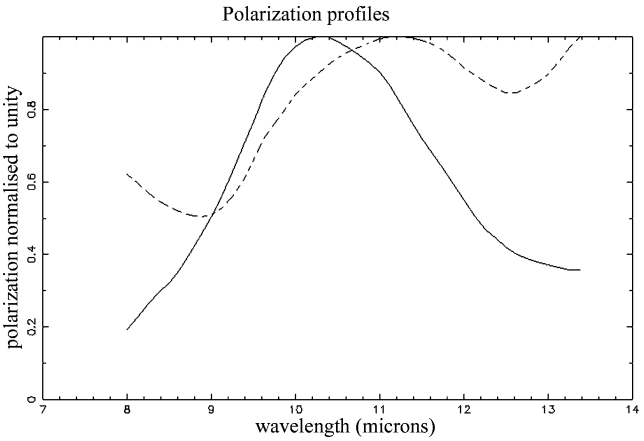

Figure 1. Absorptive polarization profile, $f_{\rm a}(\lambda)$ (solid line), taken from BN, and emissive profile, $f_{\rm e}(\lambda) \simeq f_{\rm a}(\lambda)/\tau(\lambda)$ (dashed line) (see text).

and

$$f_{\rm e}(\lambda) = p_{\rm e}(\lambda)/p_{\rm e}(\lambda_{\rm max}),$$

where $\tau(\lambda)$ is the appropriate extinction curve, here taken to be due to silicates, and derived from the observations of the Trapezium region of Orion (Gillett et al. 1975). This assumes that the grains in warm emitting regions are similar to the cold grains causing extinction, but the separation into emissive and absorptive parts depends on the gross differences between the spectra rather than their details, so that this assumption is not critical. In Fig. 1 both $f_{\rm a}(\lambda)$ and $f_{\rm e}(\lambda)$ have been normalized to unity at their respective peaks of 10.2 μm and 11.5 μm.

At this stage it is worth emphasizing the robustness of the polarimetry features. The absorptive profile from cold aligned grains is independent of the form of the source spectrum, so long as this is not itself polarized, and its position angle is constant independent of twisting of the alignment direction along the line of sight (Martin 1974). This is true provided there is no fractionation of grain chemistry along the line of sight. Absorptive polarization requires significant optical depth but its profile only becomes sensitive to optical depth when this is very large ($\tau_{\rm MIR} >$ tens). The profile of optically thin polarized emission is independent of optical depth and temperature, and its position angle remains constant provided that there are no significant temperature gradients in the emitting region.

Quite frequently both of these processes contribute to the observed polarization, and the means of testing if this is so, and evaluating the contributions from each, have been presented in Aitken (1996) and applied to the spectropolarimetry of several dozen discrete objects in SWARH. The model supposes two components: a source of radiation, $I_{\rm e}$, which either is unpolarized or has the polarization profile of optically thin silicate-like material, $p_{\rm e} \propto f_{\rm e}(\lambda)$ at $\theta_{\rm e}$, overlaid with a cold, dichroic, absorbing slab of similar material acting as an imperfect polarizer, $p_{\rm a} \propto f_{\rm a}(\lambda)$ at $\theta_{\rm a}$. With the provisos of the previous paragraph, although the field directions may twist along the line of sight, the form of $p_{\rm a}$ and $p_{\rm e}$ will not change and $\theta_{\rm a}$ and $\theta_{\rm e}$ will be the line-of-sight average and independent of λ. In terms of the Stokes parameters, the observed polarization will be

$$\begin{bmatrix} I_{\rm o} \\ Q_{\rm o} \\ U_{\rm o} \end{bmatrix} = k \begin{bmatrix} 1 & p_{\rm a}\cos 2\theta_{\rm a} & p_{\rm a}\sin 2\theta_{\rm a} \\ p_{\rm a}\cos 2\theta_{\rm a} & 1 - p_{\rm a}\sin^2 2\theta_{\rm a} & p_{\rm a}\cos 2\theta_{\rm a}\sin 2\theta_{\rm a} \\ p_{\rm a}\sin 2\theta_{\rm a} & p_{\rm a}\cos 2\theta_{\rm a}\sin 2\theta_{\rm a} & 1 - p_{\rm a}\cos^2\theta_{\rm a} \end{bmatrix} \begin{bmatrix} I_{\rm e} \\ Q_{\rm e} \\ U_{\rm e} \end{bmatrix}$$

(e.g. Serkowski 1962), where the factor k takes account of extinction and polarization on intensity.

Since all the polarizations are small (usually less than 10 per cent), we can neglect cross-products involving polarization and

$$\begin{bmatrix} I_o \\ Q_o \\ U_o \end{bmatrix} = k \begin{bmatrix} I_e \\ I_e p_a \cos 2\theta_a + Q_e \\ I_e p_a \sin 2\theta_a + U_e \end{bmatrix}.$$

Reducing to fractional quantities we then have

$$\begin{bmatrix} q_o \\ u_o \end{bmatrix} = \begin{bmatrix} p_a \cos 2\theta_a + q_e \\ p_a \sin 2\theta_a + u_e \end{bmatrix} = \begin{bmatrix} q_a + q_e \\ u_a + u_e \end{bmatrix}$$

or

$$q_o(\lambda) = q_a(\lambda) + q_e(\lambda) = A f_a(\lambda) + B f_e(\lambda)$$

and

$$u_o(\lambda) = u_a(\lambda) + u_e(\lambda) = C f_a(\lambda) + D f_e(\lambda),$$

where A, C are the values of q_a, u_a at 10.2 μm and B, D those of q_e, u_e at 11.5 μm.

Given adequate spectropolarimetric observations, then A, B, C and D can be found using an appropriate fitting procedure.

For instance, adopting a least-squares solution, we minimize

$$\chi_q^2 = \sum_i (q_{oi} - A f_{ai} - B f_{ei})^2 / \sigma_{qi}^2 \qquad (1)$$

with respect to A and B, giving

$$\frac{\partial \chi_q^2}{\partial A} = \sum_i f_{ai}(q_{oi} - A f_{ai} - B f_{ei}) / \sigma_{qi}^2 = 0,$$

$$\frac{\partial \chi_q^2}{\partial B} = \sum_i f_{ei}(q_{oi} - A f_{ai} - B f_{ei}) / \sigma_{qi}^2 = 0,$$

where the suffix i denotes the wavelength element λ_i. This leads to

$$\begin{bmatrix} \sum_i \frac{f_{ai} q_{oi}}{\sigma_{qi}^2} \\ \sum_i \frac{f_{ei} q_{oi}}{\sigma_{qi}^2} \end{bmatrix} = \begin{bmatrix} \sum_i \frac{f_{ai}^2}{\sigma_{qi}^2} & \sum_i \frac{f_{ai} f_{ei}}{\sigma_{qi}^2} \\ \sum_i \frac{f_{ei} f_{ai}}{\sigma_{qi}^2} & \sum_i \frac{f_{ei}^2}{\sigma_{qi}^2} \end{bmatrix} \begin{bmatrix} A \\ B \end{bmatrix}$$

with solution

$$\begin{bmatrix} A \\ B \end{bmatrix} = \frac{1}{\Delta} \begin{bmatrix} \sum_i \frac{f_{ei}^2}{\sigma_{qi}^2} & -\sum_i \frac{f_{ai} f_{ei}}{\sigma_{qi}^2} \\ -\sum_i \frac{f_{ei} f_{ai}}{\sigma_{qi}^2} & \sum_i \frac{f_{ai}^2}{\sigma_{qi}^2} \end{bmatrix} \begin{bmatrix} \sum_i \frac{f_{ai} q_{oi}}{\sigma_{qi}^2} \\ \sum_i \frac{f_{ei} q_{oi}}{\sigma_{qi}^2} \end{bmatrix} \qquad (2)$$

where

$$\Delta = \sum_i \frac{f_{ai}^2}{\sigma_{qi}^2} \sum_i \frac{f_{ei}^2}{\sigma_{qi}^2} - \sum_i \left(\frac{f_{ai} f_{ei}}{\sigma_{qi}^2} \right)^2.$$

In the same way, best-fitting values for C and D are found from the observed u_{oi}. Errors are found from (e.g. Bevington 1969):

$$\sigma_A^2 \sim \frac{1}{\Delta} \sum_i \frac{f_{ei}^2}{\sigma_{qi}^2}, \qquad \sigma_B^2 \sim \frac{1}{\Delta} \sum_i \frac{f_{ai}^2}{\sigma_{qi}^2},$$

and similarly for C, D substituting the errors in the u observations.

Note that A, B, C and D are the values of q_a, q_e, u_a and u_e at the wavelengths of the respective normalization, and

$$p_a(\lambda) = (A^2 + C^2)^{1/2} f_a(\lambda), \qquad \theta_a = 0.5 \tan^{-1}(C/A),$$

$$p_e(\lambda) = (B^2 + D^2)^{1/2} f_e(\lambda), \qquad \theta_e = 0.5 \tan^{-1}(D/B),$$

where again p_a and p_e refer to the respective wavelengths of normalization.

SWARH used the method of equation (2) on spectropolarimetry through 8–13 μm of a wide range of sources. In some cases, a variation of position angle with wavelength is evident, and this alone is strong evidence that there are both emissive and absorptive contributions. As an example, Fig. 2 shows, for W51 IRS2, spectra

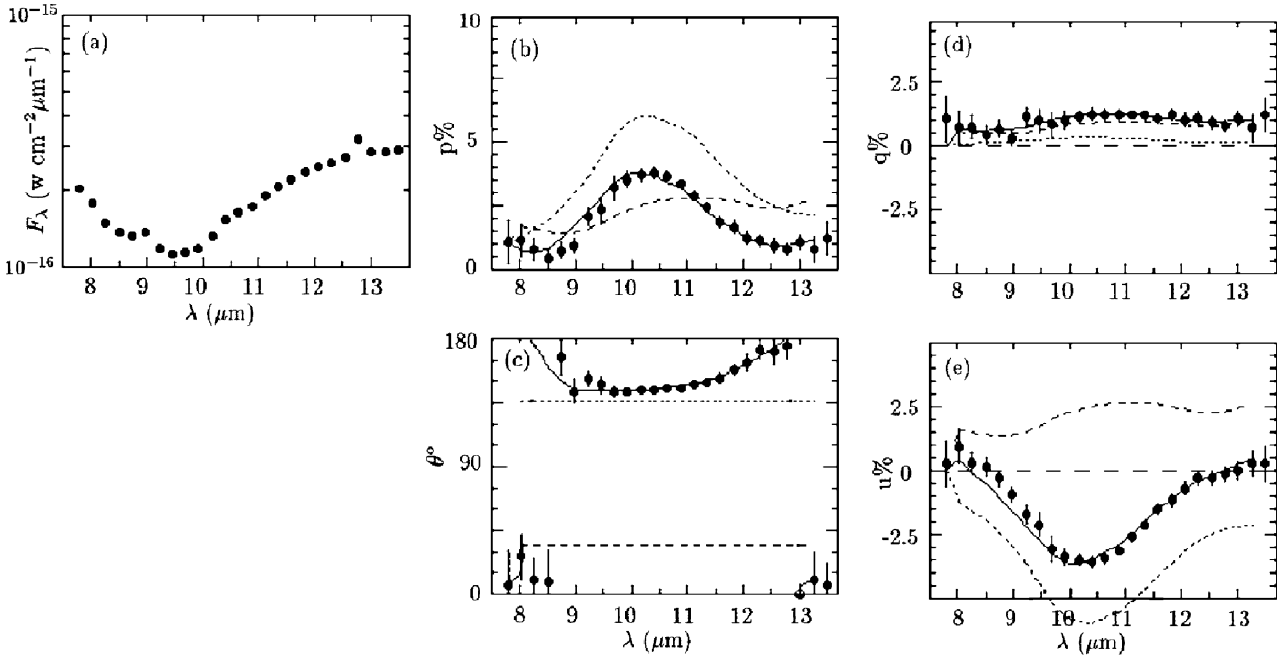

Figure 2. Spectropolarimetry of W51 (from SWARH) and fits using equation (2). Spectra of (a) intensity, (b) percentage polarization, (c) position angle, (d) and (e) Stokes percentage q and u. The solid line shows the best fit from a combination of absorption and emission, while dotted and dashed lines show their respective separate contributions.

of its intensity, polarization, position angle and the Stokes q and u parameters. In the W51 intensity spectrum there are emission lines at 9, 10.5 and 12.8 μm ([A III], [S IV] and [Ne II]). These lines are intrinsically unpolarized and will dilute the polarization, but in this case the effect is negligible. Using equation (2) SWARH find

$$p_a = 6.0 \pm 0.3 \text{ per cent}, \quad \theta_a = 137 \pm 1.4^\circ,$$

$$p_e = 2.8 \pm 0.3 \text{ per cent}, \quad \theta_e = 36 \pm 3^\circ,$$

and the reduced $\chi^2_q = 0.25$, $\chi^2_u = 1.18$. In Fig. 2 the combined fit is shown by a solid line and the separate components of p_a, θ_a and p_e, θ_e by dotted and dashed lines respectively.

It is often useful to test to what extent either single-component hypothesis is adequate through a similar procedure and χ^2 test. The least-squares solutions then are

$$A = \frac{\sum_i \left(f_{ai} q_{oi} / \sigma^2_{qi}\right)}{\sum_i \left(f^2_{ai} / \sigma^2_{qi}\right)}, \qquad C = \frac{\sum_i \left(f_{ai} u_{oi} / \sigma^2_{ui}\right)}{\sum_i \left(f^2_{ai} / \sigma^2_{ui}\right)},$$

and errors

$$\sigma^2_A = \frac{1}{\sum_i \left(1/\sigma^2_{qi}\right)}, \qquad \sigma^2_C = \frac{1}{\sum_i \left(1/\sigma^2_{ui}\right)},$$

with similar expressions for the emissive solution.

For W51 IRS2, such fits to a single component give $\chi^2_q = 0.85$, $\chi^2_u = 6.3$ for pure absorption, and $\chi^2_q = 0.23$, $\chi^2_u = 20.4$ for purely emissive polarization, in both cases much worse than for a combination of the two. Fig. 3 shows these separate fits to pure absorption by dotted lines and pure emission by dashed lines.

A negligible position angle change suggests a single polarization component, but it can also arise if both components have closely similar or orthogonal position angles. Care is needed in interpreting cases where a position angle change is dubious or non-existent, since even if the polarization is due to a single component a two-component fit should always give as good or better fit. Unless the significance of both components is high, indicating valid two components, a test to apply is to see if one of the fitted components is small or negligible with respect to the other, and it is worth comparing the χ^2 of separate fits to p_a and p_e. An example of this kind of situation is RCW38 IRS1, which SWARH assign as pure emissive polarization with a χ^2 similar to that of the combined fit; absorption alone has a significantly worse value of χ^2. The single fit in such a case also naturally gives better errors.

Sometimes the two-component fit does not overly favour one component or the other and both single-component fits give similar χ^2. Unfortunately, although there may be a well-defined position angle, there remains the $\pi/2$ ambiguity in the field direction. Even so, this may be resolved if other information is available, such as evidence for heavy extinction, as for example Mon R2 IRS2 (SWARH).

It may be of interest to consider an inventory from SWARH. Of the 40 or so sources there (excluding the Galactic Centre), roughly 70 per cent gave identifiable fits and 30 per cent of these needed two components. Roughly 20 per cent were indecisive and three objects were inconsistent with this two-component silicate hypothesis. Of the 15 Galactic Centre regions, all seen through similarly heavy interstellar extinction, all gave adequate fits with a consistently large absorptive component.

2.2 Polarimetric imaging

In observations of diffuse regions, area coverage through scanning long slits in spectropolarimetry may be impracticable or too time-consuming. In that case imaging polarimetry is required at a minimum of two wavebands and the choice of an appropriate filter set is important.

Use of a Wollaston and a mask will enable simultaneous orthogonal polarizations of small image areas to be obtained, otherwise images of orthogonal components must be sequential, with possible alignment problems. Centroiding of unresolved sources can help, but bear in mind that small resolved sources may contain polarization structure. Sometimes the presence of misalignment is betrayed by similar polarization patterns appearing in the small or unresolved sources in the image, typically a 90° change of position angle over the misalignment distance.

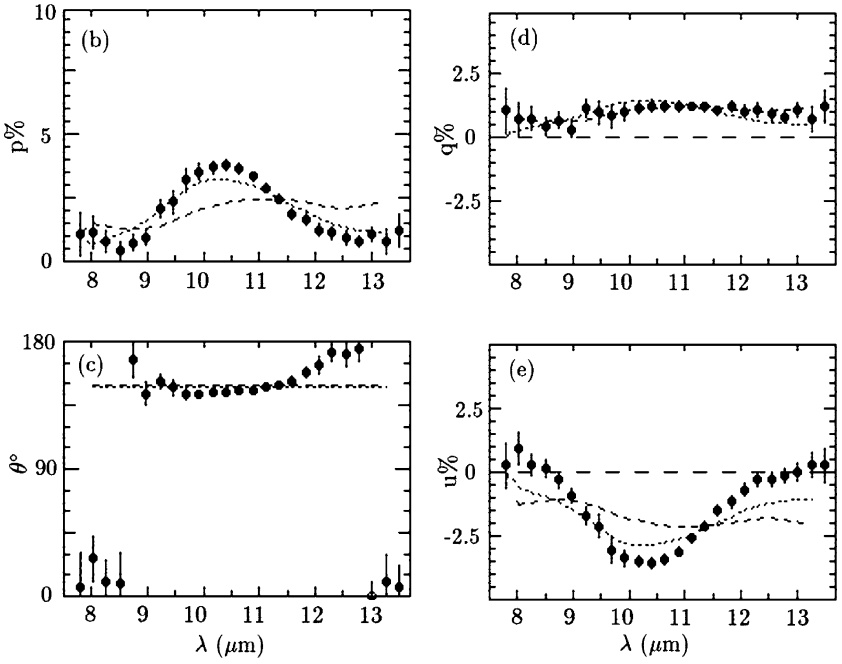

Figure 3. Spectropolarimetry of W51 with separate fits from equation (2) to pure absorptive (dotted) and pure emissive (dashed) polarization.

Table 1. Averaged polarization factors.

λ (μm)	Δλ (μm)	BN polarization f_a	f_e
8.0	1.0	0.20	0.62
8.5	1.0	0.36	0.55
8.8	1.0	0.43	0.54
9.0	1.0	0.52	0.55
9.7	1.0	0.84	0.73
10.3	1.0	0.96	0.89
10.5w	5.0	0.64	0.80
11.0	1.0	0.88	0.98
11.6	1.0	0.69	0.96
12.0	1.0	0.56	0.92
12.5	1.0	0.44	0.87
13.0	1.0	0.38	0.91

Table 1, derived from Fig. 1, shows the relative values of the absorption and emission polarization profiles at some sample wavebands with typical bandwidth of 1 μm and a broad-band filter covering the 8–13 μm window.

For wavelength pairs λ_1 and λ_2, we have the simultaneous equations

$$\begin{bmatrix} q_{o1} \\ q_{o2} \end{bmatrix} = \begin{bmatrix} f_{a1} & f_{e1} \\ f_{a2} & f_{e2} \end{bmatrix} \begin{bmatrix} A \\ B \end{bmatrix} \qquad 2.2$$

with solution

$$\begin{bmatrix} A \\ B \end{bmatrix} = \frac{1}{\Delta_{12}} \begin{bmatrix} f_{e2} & -f_{e1} \\ -f_{a2} & f_{a1} \end{bmatrix} \begin{bmatrix} q_{o1} \\ q_{o2} \end{bmatrix}, \qquad (3)$$

where

$$\Delta_{12} = f_{a1} f_{e2} - f_{a2} f_{e1},$$

with similar solutions for C, D, replacing the q with u. If $\Delta_{12} = 0$ then (3) is not a solution, and the best solutions are expected when the choice of filters makes $|\Delta_{12}|$ large, equivalently when they maximize the difference between the two wavebands. Table 2 shows the values of Δ_{12} for the filter selection shown in Table 1.

The effect of observational errors is assessed in the usual way:

$$\mathrm{d}A^2 = \left(\frac{\partial A}{\partial q_{o1}}\mathrm{d}q_{o1}\right)^2 + \left(\frac{\partial A}{\partial q_{o2}}\mathrm{d}q_{o2}\right)^2 = \left[(f_{e2}\mathrm{d}q_{o1})^2 + (f_{e1}\mathrm{d}q_{o2})^2\right] \Big/ (\Delta_{12})^2, \qquad (4)$$

and similarly for dB, dC and dD.

Applying this to W51 IRS2 and binning data from SWARH into 1-μm bins, we have

$p_{12.5} = 0.97 \pm 0.2$ per cent, $\quad \theta_{12.5} = 172 \pm 6^\circ$,

($q_{12.5} = 0.94 \pm 0.2$ per cent, $\quad u_{12.5} = -0.25 \pm 0.2$ per cent),

$p_{10.3} = 3.6 \pm 0.15$ per cent, $\quad \theta_{10.3} = 144 \pm 1.5^\circ$,

($q_{10.3} = 1.1 \pm 0.15$ per cent, $\quad u_{10.3} = -3.4 \pm 0.15$ per cent).

Using these data in equation (3) we get

$p_a = 6.2 \pm 0.5$ per cent, $\quad \theta_a = 136 \pm 2^\circ$,

$p_e = 3.0 \pm 0.5$ per cent, $\quad \theta_e = 36 \pm 4^\circ$.

The results agree comfortably within the errors with the full spectropolarimetric treatment, but there is no χ^2 check on consistency with the two-component hypothesis. One way is to use other wavebands as a consistency check: e.g. replacing the 12.5-μm data with 8.5 μm:

$p_{8.5} = 0.55 \pm 0.25$ per cent, $\quad \theta_{8.5} = 176 \pm 12^\circ$,

($q_{8.5} = 0.55 \pm 0.25$ per cent, $\quad u_{8.5} = -0.07 \pm 0.25$ per cent),

giving

$p_a = 8.8 \pm 1.1$ per cent, $\quad \theta_a = 137 \pm 4^\circ$,

$p_e = 5.6 \pm 1.2$ per cent, $\quad \theta_e = 42 \pm 6^\circ$.

The two results are clearly consistent with each other and with the spectropolarimetric results, and the wavelength pairs have similar values of $|\Delta_{12}|$, while the three wavebands are widely spread. Inspection of Table 2 shows that combinations of the middle of the waveband with its edges give the largest values of $|\Delta_{12}|$ which maximize the change between f_a and f_e; unfortunately the largest values of $|\Delta_{12}|$ involve the extreme edges of the 10-μm window where the transmission is poor, and allowance should be made for this. The wavebands used in this section are a suitable selection.

If we use equation (2) for the three wavelengths above we get

$p_a = 5.8 \pm 0.4$ per cent, $\quad \theta_a = 136 \pm 2^\circ$,

$p_e = 2.9 \pm 0.4$ per cent, $\quad \theta_e = 35 \pm 3^\circ$,

with $\chi^2_q = 0.03$ and $\chi^2_u = 2.3$.

In those cases where the two (or more) observed position angles agree within their errors, we can test whether or not the

Table 2. Δ_{12}.

	λ_1 (μm)										
λ_2 (μm)	8.5	8.8	9.0	9.7	10.3	10.5w	11.0	11.6	12.0	12.5	13.0
8.0	0.113	0.159	0.212	0.375	0.417	0.237	0.350	0.236	0.163	0.099	0.054
8.5	–	0.042	0.088	0.199	0.208	0.064	0.132	0.034	−0.023	−0.071	−0.119
8.8		–	0.044	0.140	0.135	0.002	0.054	0.040	−0.093	−0.136	−0.186
9.0			–	0.082	0.062	0.064	−0.026	−0.120	−0.170	−0.210	−0.264
9.7				–	0.047	−0.208	−0.181	−0.303	−0.364	−0.410	−0.487
10.3					–	−0.198	−0.158	−0.307	−0.385	−0.444	−0.535
10.5w						–	0.077	−0.062	−0.141	−0.205	−0.278
11.0							–	−0.169	−0.261	−0.334	−0.428
11.6								–	−0.097	−0.178	−0.263
12.0									–	−0.082	−0.160
12.5										–	−0.070

polarizations are in the ratio of either f_{a1}/f_{a2} or f_{e1}/f_{e2} within their respective errors. Then if, for example, pure absorption is favoured,

$$A = \frac{f_{a1}q_{o1}/\sigma_{q1}^2 + f_{a2}q_{o2}/\sigma_{q2}^2}{f_{a1}^2/\sigma_{q1}^2 + f_{a2}^2/\sigma_{q2}^2},$$

with similar expressions for C, from which the solutions for p_a and θ_a follow with substantially better errors than for a two-component fit.

3 CONCLUSIONS

Polarization in the mid-infrared can arise through emission or absorption by aligned grains, or a combination of both. These components are respectively at right angles or parallel to the projection of grain spin axes on the plane of the sky, and can lead to confusion in the determination of magnetic field direction from polarimetry. Polarization at a single wavelength in this spectral region cannot resolve this ambiguity; the field direction is completely undetermined unless other information is available. Procedures for identifying and separating these components from spectropolarimetry or polarimetric imaging at a minimum of two wavebands are presented here.

REFERENCES

Aitken D. K., 1996, in Roberge W. G., Whittett D. C. B., eds, ASP Conf. Ser. Vol. 97, Polarimetry of the Interstellar Medium. Astron. Soc. Pac., San Francisco, p. 225
Aitken D. K., Smith C. H., Roche P. F., 1989, MNRAS, 236, 919
Bevington P. R., 1969, Data reduction and error analysis for the physical sciences. McGraw-Hill, Columbus, Ch. 6.
Dolginov A. Z., Mytrophanov L. G., 1976, Ap&SS, 43, 291
Draine B. T., Lee H. M., 1984, ApJ, 285, 89
Gillett F. C., Kleinmann D. E., Wright E. L., Capps R. W., 1975, ApJ, 198, L65
Landau L. D., Lifshitz E. M., 1960, in Electrodynamics of Continuous Media. Addison-Wesley, Reading, MA, p. 144
Martin P. G., 1974, ApJ, 197, 461
Serkowski K., 1962, Adv. Astron. Astrophys., 1, 289
Smith C. H., Wright C. M., Aitken D. K., Roche P. F., Hough J. H., 2000, MNRAS, 312, 327 (SWARH)

This paper has been typeset from a TEX/LATEX file prepared by the author.